Charged Particle Behavior in Low-Frequency Geomagnetic Pulsations
4. Compressional Waves

MARGARET G. KIVELSON

Institute of Geophysics and Planetary Physics, University of California, Los Angeles
Department of Earth and Space Sciences, University of California, Los Angeles

DAVID J. SOUTHWOOD

Institute of Geophysics and Planetary Physics, University of California, Los Angeles
Department of Physics, Imperial College of Science and Technology, London

In this fourth paper of a series concerning charged particle behavior in ultralow frequency waves in the terrestrial magnetosphere, we examine the particle flux response expected in waves with a strong compressional magnetic component. Two effects, which we label betatron and mirror, dominate the behavior expected for nonresonant particles with the mirror effect expected in most circumstances. Resonant behavior is a strong function of signal symmetry, much as discussed in earlier papers. We conclude by examining recently published observations of particle flux oscillations associated with compressional signals.

1. INTRODUCTION

In this paper we extend studies presented earlier by *Southwood and Kivelson* [1981, 1982] and *Kivelson and Southwood* [1983]. Those earlier papers, referred to henceforth as papers 1, 2, and 3, respectively, put much emphasis on the properties of large-scale transverse magnetospheric ULF waves. Here we focus on compressional waves, i.e., waves with significant magnetic perturbations aligned with the background field, **B**.

Long-period (≥ 2 min) ultralow-frequency (ULF) compressional waves in the magnetosphere near synchronous orbit have been surveyed by *Barfield and McPherron* [1978], *Kremser et al.* [1981], and *Higbie and McPherron* [1982]. Specific events have been described by others (see references in the work of *Southwood* [1980]), most recently by *Walker et al.* [1982, 1983]. A distinct type of ULF magnetic compressional signal is found in magnetotail vortex events [*Saunders et al.*, 1981, 1983a, b]. Events already described in the literature provide considerable data illustrating the behavior of charged particles in compressional waves, and we will show how they relate to some of the theoretical ideas to be discussed here.

In interpreting the data, one would like to understand the relation between wave electromagnetic properties and the energy and pitch angle dependent phase and amplitude of particle flux oscillations. All of these must be understood in terms of both the local and large-scale structure of the waves. Ultimately, the purpose of the analysis is to identify the wave generation mechanism and to show how these low-frequency waves act to redistribute energy among the plasma populations of the magnetosphere and the ionosphere. However, such a goal is long term; our explicit aim in this paper is to describe the possible classes of particle flux behavior in a ULF signal with a significant magnetic compressional component.

This paper should be read as part of a series (papers 1–3), so we will not repeat work we have already presented. In particular, we do not treat the gyrophase-dependent effects that dominate low-energy charged particle response. These are

dealt with in paper 1, and are important for particles whose bounce frequency, ω_b, is less than the wave frequency, ω. Neither do we treat the finite Larmor radius effects examined in detail in paper 3, although one should note that they are important in observed compressional signals. In this paper we restrict ourselves to treating particles whose Larmor radii are much less than any scale of wave signal variation.

2. COMPRESSIONAL EFFECTS

The presence of the fluctuating magnetic field component, $b_{\parallel}$, parallel to **B** produces specific effects on particle flux not considered in paper 1, and we examine those first. An estimate of when they dominate the contribution of the associated wave electric field which can be treated just as in our earlier papers is given in a later section.

We describe the particle response in terms of the phase space distribution function, f, a function of μ, W, and L, where μ and W are a particle's first adiabatic invariant and energy and L is the flux tube coordinate, equal to the radial distance in earth radii (R_E) to the equatorial crossing point of the unperturbed flux tube. We assume that both spatial and temporal scales are sufficiently large that $\mu = W_\perp/B_T$ is conserved. Here $W_\perp$ is the perpendicular kinetic energy and the total magnetic field is $\mathbf{B}_T = \mathbf{B} + \mathbf{b}$.

In the linear approximation, the perturbation in f produced by an arbitrary compressional signal has the form implied by the Liouville theorem

$$\delta f(\mu, W, L) = -\delta W \frac{\partial f}{\partial W} - \delta L \frac{\partial f}{\partial L} - \frac{\mu b_{\parallel}}{B} \frac{\partial f}{\partial \mu} \quad (1)$$

The first two terms represent the acceleration and the radial displacement of a particle in the electromagnetic fields of the wave. The final term arises from the fact that, with μ conserved, the velocity space coordinates scale with the total magnetic field. The corresponding change in f represents the exclusion of particles from regions of stronger magnetic field by a quasi-static compressive field perturbation. We label this term the "mirror effect" and explain it more fully in the appendix, which also reviews the relative roles of the first and third terms.

The particle energy change produced by the wave compression, $b_{||}$, is

$$\dot{W} = \mu \frac{\partial b_{||}}{\partial t} \qquad (2)$$

in a linear approximation. The compressional signal also produces a guiding center drift which we obtain by assuming **B** to be locally axisymmetric as we did in paper 1. Then we expect that the initial, steady state distribution is independent of longitude, ϕ, but dependent on L. Thus we are interested in the drift in the L direction produced by $b_{||}$

$$\delta v_L = \mathbf{B} \times \mu \nabla_\phi b_{||}/qB^2 \qquad (3)$$

where q is the particle's charge. The rate of change of L is given by [cf. Dungey, 1965]

$$\dot{L} = \delta v_L \cdot \nabla L = -\mu \frac{\partial b_{||}}{\partial \phi} \bigg/ qB_e LR_E^2 \qquad (4)$$

where ϕ is measured positive eastward, and B_e is the equatorial field.

If $b_{||} \propto \exp i(m\phi - \omega t)$, then (2) and (4) imply

$$\frac{\delta W}{\delta L} = qB_e LR_E^2 \omega/m \qquad (5)$$

as both $\dot{W}$ and $\dot{L}$ are proportional to $b_{||}$. We then have

$$\delta f = -\delta W \left(\frac{\partial f}{\partial W} + \frac{m}{q\omega B_e LR_E^2} \frac{\partial f}{\partial L} \right) - \frac{\mu b_{||}}{B} \frac{\partial f}{\partial \mu} \qquad (6)$$

As a general rule in the remainder of this paper, we shall assume for purposes of comparison that $(\partial f/\partial \mu)B^{-1}$ and $(\partial f/\partial W)$ are of the same order.

It is convenient to reexpress (6) in terms of the ratio

$$-(\partial f/\partial L)/(\partial f/\partial W)qB_e LR_E^2 = \omega^* \qquad (7)$$

Then (6) becomes

$$\delta f = -\delta W \frac{\partial f}{\partial W} \left(1 - \frac{m\omega^*}{\omega} \right) - \frac{\mu b_{||}}{B} \frac{\partial f}{\partial \mu} \qquad (8)$$

For Maxwellian distribution with a density gradient, ω^* is the diamagnetic drift frequency (see, e.g., Hasegawa [1975]). In that special case, ω^* is proportional to distribution temperature, but in general, the parameter ω^* defined here should vary with the energy of the part of distribution that is examined.

Most theoretical treatments of particles in compressional waves in the magnetosphere [e.g., Hasegawa, 1975; Lin and Parks, 1978; Walker et al., 1982] are based on straight field geometry and thus do not treat correctly the responses of particles bouncing in a curved background field. Southwood [1973] formulates the correct description introducing the bounce phase defined in terms of $\omega_b/2\pi$, the bounce frequency, by

$$\theta = \int_{eq}^s ds\, \omega_b/v_{||} \qquad (9)$$

where s is distance along the field direction. θ is measured from the equator and equals 0 or π as a particle moves northward or southward, respectively, through the equator. The rate of change of a particle's energy can be expressed as a Fourier series in θ,

$$\dot{W} = \sum_{N=-\infty}^{\infty} \dot{W}_N e^{iN\theta} \exp i(m\tilde{\omega}_d - \omega)t \qquad (10)$$

where $\tilde{\omega}_d$ is the particle's bounce-averaged longitudinal drift rate. The coefficients $\dot{W}_N$ are independent of bounce phase, and $|\dot{W}_N|^2$ represents the power seen by the particle at the Nth harmonic of its bounce frequency.

Now from (2),

$$\delta W = \int_{orbit} \dot{W} dt = -i\omega\mu \int_{orbit} b_{||}\, dt \qquad (11)$$

where the orbit consists of a drift through longitude and a bounce back and forth through latitude, and

$$\delta W = \sum_{N=-\infty}^{\infty} \frac{\omega\mu b_{||N} e^{i(m\bar{\phi}-\omega t)} e^{iN\theta}}{(\omega - m\tilde{\omega}_d - N\omega_b)} \qquad (12)$$

where $\bar{\phi} = \tilde{\omega}_d t + \phi_0$. Equations (8) and (12) give the form we seek for the response of the particle distribution function to a compressional signal:

$$\delta f = -\sum_{N=0}^{\infty} \left(\frac{\mu b_{||N}(\omega - \omega^*)}{(\omega - m\tilde{\omega}_d - N\omega_b)} e^{i(m\bar{\phi}-\omega t)} e^{iN\theta} \frac{\partial f}{\partial W} \right) - \frac{\mu b_{||}}{B} \frac{\partial f}{\partial \mu} \qquad (13)$$

The form of the response (13) depends critically on the symmetry of the wave perturbation along the field line, as well as on the relative magnitudes of four frequencies (ω, ω^*, ω_d, ω_b). Furthermore, the case of resonant particles for which

$$\omega = m\omega_d + N\omega_b \qquad (14)$$

3. EQUATORIAL PARTICLE RESPONSE

For particles with 90° pitch angle located at the magnetic field equator (minimum in B), the bounce phase expansion is unnecessary and (13) adopts a simpler form which we can use to introduce ideas we shall also use in our general treatment. In this case,

$$\delta f = -\frac{(\omega - m\omega^*)}{(\omega - m\omega_d)} \mu b_{||} \frac{\partial f}{\partial W} - \frac{\mu b_{||}}{B} \frac{\partial f}{\partial \mu} \qquad (15)$$

The relative sizes of three frequencies determine the relative importance of the two terms in (15) and thus the nature of the particle response. Limiting cases are described in the following subsections. The inequalities are energy dependent, so, in general, they will hold only over part of any given distribution.

3.1. $\omega \gg m\omega^*, m\omega_d$

In the limit of large ω, one has to a good approximation

$$\delta f = -\mu b_{||} \left(\frac{\partial f}{\partial W} + \frac{1}{B} \frac{\partial f}{\partial \mu} \right) \qquad (16)$$

Equation (16), identical with (A15), represents what we call the betatron effect, the response when perpendicular heating is dominant. In this case, perpendicular energy is changing, but parallel energy is not. Indeed, $\omega \gg m\omega^*$, $m\omega_d$ is for 90° particles a specific statement of the general condition (A8) under which perpendicular acceleration dominates.

3.2. $m\omega_d \gg \omega \gg m\omega^*$

The assumption $\omega \gg m\omega^*$ implies spatial distribution gradients are not important, but $m\omega_d \gg \omega$ implies that the particle drifts through a longitudinal wavelength in a time short in comparison with the wave period, so the signal appears to the particle as quasi-static but spatially varying. The energy

change is down by a factor of $\omega/m\omega_d$ on the previous case, and

$$\delta f = \frac{\omega\mu b_{||}}{m\omega_d}\frac{\partial f}{\partial W} - \frac{\mu b_{||}}{B}\frac{\partial f}{\partial\mu} \simeq -\frac{\mu b_{||}}{B}\frac{\partial f}{\partial\mu} \qquad (17)$$

Equations (17) and (A13) are the same and represent what we call the mirror effect, which dominates when the signal seen by a particle is quasi-static (condition (A5) of the appendix).

3.3. $\omega = m\omega^*$

The mirror effect is completely dominant in one further case. If

$$\omega = m\omega^* \qquad (18)$$

then

$$\delta f = -\mu b_{||}\frac{\partial f}{\partial\mu}$$

As we noted earlier, ω^* will normally vary with energy and thus (18) would hold only over a limited range of energies. However, should the radial density gradient in the distribution be approximately independent of energy, (18) could hold (for a signal with appropriate frequency) for the entire distribution, but then only for one species as the sign of ω^* is charge dependent.

3.4. $\omega^* = \omega_d$

In much of the magnetosphere the distribution is one set up by injection across L shells by an adiabatic (μ, J conserving) convection or diffusion process. In the case of equatorial particles, $J = 0$. If particles have been injected from large L regions, the particle energy will have varied as

$$\frac{\partial W_\perp}{\partial L} = \frac{\partial W}{\partial L} = \mu\frac{\partial B}{\partial L} \qquad (19)$$

If the injection process is fairly steady, and losses are weak, the inward gradient in distribution function, f, should satisfy

$$\frac{\partial f}{\partial L} = \mu\frac{\partial B}{\partial L}\frac{\partial f}{\partial W} \qquad (20)$$

From (20) and the definition of ω^*, (7), it follows that for an adiabatic distribution

$$\omega^* = -\mu\frac{\partial B}{\partial L}\bigg/qB_eLR_E^2 = \text{angular } \nabla B \text{ drift} = \omega_d \qquad (21)$$

In this case, from (15),

$$\delta f = -\mu b_{||}\left(\frac{\partial f}{\partial W} + \frac{1}{B}\frac{\partial f}{\partial\mu}\right) \qquad (22)$$

i.e., perpendicular energy change dominates as in (A15). Equation (22) holds for any adiabatically injected distribution of equatorially trapped particles, even if drift resonance occurs (see below).

3.5. $\omega = m\omega_d$

The integration procedure used to derive (12) is invalid if

$$\omega = m\omega_d \qquad (23)$$

In paper 1, suitable expressions for resonant particle energy and L shell changes were obtained by assuming a slowly growing wave amplitude from $t = -\infty$. Following the same procedure as in paper 1, one finds (equation (11), paper 1)

$$\langle\delta W_{res}\rangle = \frac{-i\pi\mu b_{||}}{4}\frac{v_{res}}{\Delta v_D} \qquad (24)$$

where $\langle\delta W_{res}\rangle$ is the mean energy response in a detector whose energy bandwidth corresponds to a spread in velocity, $2\Delta v_D$, centered on the resonant energy. A factor of 4 has been introduced here. This was erroneously omitted from paper 1. One factor of 2 is from the velocity bandwidth $2\Delta v_D$. The second is because $\partial\omega_d/\partial v$ is $2\omega_d/v$ not ω_d/v.

The distribution function perturbation produced is

$$\langle\delta f_{res}\rangle = \frac{i\pi\mu b_{||}v_{res}}{4\Delta v_D\omega_d}(\omega_d - \omega^*)\frac{\partial f}{\partial W} - \mu b_{||}\left(\frac{\partial f}{\partial W} + \frac{1}{B}\frac{\partial f}{\partial\mu}\right) \qquad (25)$$

Provided the detector bandwidth is not too broad (i.e., $\Delta v_D < v_{res}$) and that $\omega_d \neq \omega^*$, the first term on the right-hand side of (25) will be the more important. The presence of the factor i multiplying the first term shows that just at resonance there will be a 90° phase difference between $b_{||}$ and the distribution perturbation, a distinct resonance signature. For energies near the resonant energy, (15) shows that the relative phase of the signal $b_{||}$ and the distribution function (and therefore flux) oscillation changes by π as the energy considered is varied through the resonance energy. The sense of the phase switch depends on the sign of $(\omega^* - \omega_d)$ and thus depends on the relative importance of spatial and phase space gradients.

4. BOUNCING PARTICLES

The cases outlined in section 3 all fit fairly well into three identifiable categories of behavior. They are (1) the mirror effect (quasi-static changes in $W_{||}$ and $W_\perp$ but not in W as the particles respond to spatially changing wave fields), (2) the betatron effect (changes in $W_\perp$ alone as the particles respond to temporally changing wave fields), (3) the resonance effect (dominant for particles whose east-west drift speed matches the wave perpendicular phase speed). In addition, one should note that in the limit of large ω^* (not considered in section 3), changes in f arise from the cross-L drift effect because of the strong radial gradients implicit if ω^* is large. The same categories can apply to particles with finite amplitude bounce orbits but with complications. First, the response depends on the symmetry of the wave perturbation along the field line. Second, bounce resonance as well as drift resonance can occur. First, we take up the question of symmetry.

For a disturbance that is symmetric about the magnetic equator, only even terms contribute to the summation in (12) and

$$\delta W = \sum_{l=0}^{\infty}(-i\omega\mu)b_{||2l}e^{i(m\tilde{\varphi} - \omega t)}$$

$$\cdot\left[\frac{i(\omega - m\tilde{\omega}_d)\cos 2l\theta - 2l\omega_b\sin 2l\theta}{(\omega - m\tilde{\omega}_d)^2 - (2l\omega_b)^2}\right] \qquad (26)$$

For an antisymmetric disturbance, an analogous expression can be derived involving only odd harmonics, $(2l + 1)\omega_b$, of the bounce frequency and associated odd bounce Fourier coefficients $b_{||(2l+1)}$.

Noting that this paper exclusively concerns particles for which $\omega_b > \omega$ and further limiting our consideration of the energy change (26) to nonresonant particles (so that the denominator is nonvanishing), we can note that the $(2l)$th term is smaller than the first term by a factor of at least

$$[(\omega - m\tilde{\omega}_d)/2l\omega_b]|b_{||2l}/b_{||0}| \qquad (27)$$

A signal that varies slowly along **B** and hence slowly with bounce phase typically satisfies

$$|b_{\|2t}/b_{\|0}| \ll 1 \tag{28}$$

The inequality (28) is stronger than we need in order to assure that higher-order terms in (26) are small and that the change of particle energy is well approximated by

$$\delta W = \omega\mu b_{\|0}/(\omega - m\tilde{\omega}_d) \tag{29}$$

where the remaining phase factor has been absorbed in $b_{\|0}$. By definition, $b_{\|0}$ is the bounce-averaged value of $b_{\|}$ seen by the particle

$$b_{\|0} = \frac{1}{2\pi}\int_0^{2\pi} d\theta\; b_{\|} = \frac{\omega_b}{2\pi}\oint \frac{ds}{v_{\|}} b_{\|} \tag{30}$$

For nonresonant particles in an antisymmetric disturbance that varies slowly along **B**, it is sensible to approximate δW by ignoring higher-order harmonics in a similar way. Thus we write

$$\delta W \simeq (-i\omega\mu)b_{\|1}e^{i(m\tilde{\varphi}-\omega t)}\frac{i(\omega - m\tilde{\omega}_d)\sin\theta - \omega_b\cos\theta}{(\omega - m\tilde{\omega}_d)^2 - \omega_b^2} \tag{31}$$

(cf. equation (20b) of paper 1).

The distribution function differs for a symmetric or an antisymmetric disturbance because of the different forms of δW ((29) or (31)). For an antisymmetric disturbance, provided ω, $m\tilde{\omega}_d \ll \omega_b$, δW is small, of the order of $\omega\mu b_{\|}/\omega_b$, yielding from (8)

$$\delta f = -\frac{\mu b_{\|}}{B}\frac{\partial f}{\partial \mu} \tag{32}$$

The mirror effect is thus dominant.

For a symmetric disturbance, (29) and (8) yield

$$\delta f = -\left(\frac{\omega - m\omega^*}{\omega - m\tilde{\omega}_d}\right)\mu b_{\|0}\frac{\partial f}{\partial W} - \frac{\mu b_{\|}}{B}\frac{\partial f}{\partial \mu} \tag{33}$$

Equation (33) appears similar to (15), and for particles mirroring near the equator, its consequences are analogous to those of section 3. For particles with small equatorial pitch angles that thus mirror far off the equator, the mirror effect dominates when

$$m\tilde{\omega}_d \gg \omega, m\omega^* \tag{34a}$$

or

$$\omega = m\omega^* \tag{34b}$$

However, when either

$$\omega > m\tilde{\omega}_d, m\omega^* \tag{35a}$$

or

$$\omega^* = \omega_d \tag{35b}$$

(the latter equality implying an adiabatic distribution), (33) becomes

$$\delta f \simeq -\mu b_{\|0}\frac{\partial f}{\partial W} - \frac{\mu b_{\|}}{B}\frac{\partial f}{\partial \mu} \tag{36}$$

The response depends on the relative size of $|b_{\|0}|$ and $|b_{\|}|$. Now, $b_{\|}$ is a local quantity, being measured at the position where the wave is detected. But $b_{\|0}$ is not a local quantity; it is bounce averaged and thus independent of latitude. Thus the response described by (36) is pitch angle dependent. Figure 1 shows an idealized instance of two bouncing particles in com-

pressional wave at the equator. The amplitude, $b_{\|}$, is plotted schematically versus distance along **B**. It peaks at the equator. Particles 1 and 2 are envisaged as bouncing between mirror points m_1 and m_2, respectively. Sketched in are values for $b_{\|0}$ for the two particles. Evidently, near the equator, $|b_{\|}|$ exceeds both $|b_{\|01}|$ and $|b_{\|02}|$; however, only for the small pitch angle particle 2 does one have the strong inequality $|b_{\|}| \gg |b_{\|02}|$ needed for the final term of (36) to dominate. One concludes that near the equator, the betatron effect will characterize the response of locally mirroring particles and the mirror effect will be strongly evident in the smaller pitch angle particles. Far off the equator near the mirror point of particle 2, $|b_{\|02}| > |b_{\|}|$ and thus the energization term will be dominant in (36). Hence which term dominates the right-hand side of (36) is a function of pitch angle and the latitude of measurement and the latitudinal variation of the signal amplitude.

5. BOUNCE RESONANCE

In principle, a resonant response is experienced by any particle whose bounce and drift frequency satisfy [Southwood et al., 1969]

$$\omega - m\tilde{\omega}_d = N\omega_b \tag{37}$$

where N is an integer. In particular, drift resonance, where $N = 0$, occurs for signals that are symmetric about the equator. For antisymmetric signals with long parallel wavelength, the most important resonances are $N = \pm 1$. Generally, in this latter case, there are two resonant energies for given ω and m, a high-energy resonance where $m\tilde{\omega}_d \simeq \omega_b$, and a low-energy resonance where $\omega \simeq \omega_b$ [Southwood et al., 1969]. On order of magnitude grounds, $m\tilde{\omega}_d \simeq \omega_b$ implies the east-west wavelength is of the order of the particle Larmor radius. In contrast, the low-energy condition $\omega \simeq \omega_b$ marks the point where the effects examined in this paper cease to be as important as gyration acceleration. Thus (cf. the introduction, section 1) the bounce resonant particle energies bracket the range of energies in which we feel compressional effects are important.

Drift resonance can be dealt with by direct analogy to the equatorial mirroring case described in section 3. By analogy with (25), one finds

$$\langle\delta f_{res}\rangle = \frac{i\pi\mu b_{\|0}v_{res}}{4\Delta v_D\tilde{\omega}_d}(\tilde{\omega}_d - \omega^*)\frac{\partial f}{\partial W} - \mu b_{\|0}\frac{\partial f}{\partial W} - \frac{\mu b_{\|}}{B}\frac{\partial f}{\partial \mu} \tag{38}$$

for the mean response in a detector whose energy window straddles the resonant energy. Again, the bounce average of $b_{\|}$ has replaced the local value of $b_{\|}$ in the term of (25) that describes resonant response of 90° equatorially mirroring particles and $\tilde{\omega}_d$ has replaced ω_d. Generally, near resonance the first term dominates in (38). As we noted before, an adiabatic distribution is exceptional. For such a distribution, $\omega^* = \tilde{\omega}_d$, the resonant term vanishes, and the final term on the right side implies that the response parallels that of the nonresonant particles given by (36). The particle distribution response near a resonant energy in an antisymmetric disturbance is dealt with similarly to the drift resonance case. Once again more detail is provided in paper 1. One finds

$$\langle\delta f_{res}\rangle = -\frac{i\pi\mu b_{\|1}(\omega - m\omega^*)}{2m\tilde{\omega}_d \pm \omega_b}\frac{v_{res}}{2\Delta v_D}\frac{\partial f}{\partial W} - \frac{\mu b_{\|}}{B}\frac{\partial f}{\partial \mu} \tag{39}$$

Provided the detector has a narrow enough energy band ($\Delta v_D \gg v_{res}$), the resonant term should dominate and be in quadrature with signals in neighboring nonresonant channels much as we described in section 3. As we described in papers 2
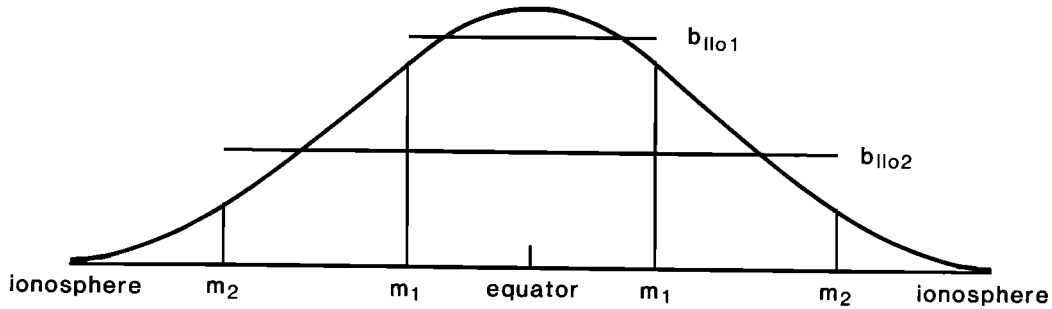
Fig. 1. Schematic of $b_{||}$ variation along a field line from ionosphere through equator to conjugate ionosphere. Points labeled m_1, m_2 indicate mirror points of a large and small equatorial pitch angle particle, respectively. The lines $b_{||o1}$ and $b_{||o2}$ indicate notional values of $b_{||o}$ for the two particles.

and 3 in this instance, very strong anisotropies develop in detectors looking along or antiparallel to **B**.

6. ELECTRIC FIELD EFFECTS

In the preceding sections we have outlined effects directly produced by a compressional magnetic signal. We have ignored the electric field associated with any time-varying magnetic signal other than the effect of curl **E** acting about the circle of gyration implicit in the acceleration equation (2) [Northrop, 1963]. In this section we describe the modification arising from the electric field and consider when they are or are not important.

Faraday's law gives

$$\frac{\partial b_{||}}{\partial t} = -(\nabla \times \mathbf{E}) \cdot \frac{\mathbf{B}}{B} \tag{40}$$

After some rearrangement, and with $E_{||} = 0$, this can be written in terms of the field line velocity $\mathbf{E} \times \mathbf{B}/B^2$ [Southwood, 1973]:

$$\frac{\partial b_{||}}{\partial t} = -B\nabla \cdot \left(\frac{\mathbf{E} \times \mathbf{B}}{B^2}\right) - \frac{\mathbf{E} \times \mathbf{B}}{B^2} \cdot \left(\nabla B - \frac{\mathbf{R}_c B}{R_c^2}\right) \tag{41}$$

where $\mathbf{R}_c$ is the field curvature vector equal to $-\hat{e} \cdot \nabla e$ for $\hat{e} = \mathbf{B}/|B|$. The relation

$$\frac{\mathbf{E} \times \mathbf{B}}{B^2} = \frac{\partial \boldsymbol{\xi}}{\partial t} \tag{42}$$

serves to define a field displacement, $\boldsymbol{\xi}$, and then one has

$$b_{||} = -(\nabla \cdot \boldsymbol{\xi})B - \boldsymbol{\xi} \cdot \nabla B + \frac{\boldsymbol{\xi} \cdot \mathbf{R}_c B}{R_c^2} \tag{43}$$

Now, as was clear from the preceding sections as well as from papers 1-3, we are concerned with effects that change perpendicular and parallel energy and/or move particles in the meridian, in L. The relevant components of **E** and $\boldsymbol{\xi}$ are E_ϕ and ξ_n (n denoting the component in the meridian perpendicular to **B**). The electric field requires that additional terms, $\dot{W}_E$ and $\dot{L}_E$, be added to (2) and (4), respectively, so that the energy change becomes $\dot{W} + \dot{W}_E$ and the radial velocity becomes $\dot{L} + \dot{L}_E$. These new terms can be written (paper 1) as

$$\dot{W}_E = qE_\phi v_d = \boldsymbol{\xi} \cdot \left[\mu\nabla B - 2(W - \mu B)\frac{\mathbf{R}_c}{R_c^2}\right] \tag{44}$$

$$\dot{L}_E = \frac{\mathbf{E} \times \mathbf{B}}{B^2} \cdot \nabla L + \frac{v_{||}\mathbf{b} \cdot \nabla L}{B}$$

$$= \frac{d}{dt}(\boldsymbol{\xi} \cdot \nabla L) + \frac{m\dot{W}_E}{q\omega B_e L R_E^2} \tag{45}$$

The first term on the right side of (45) is the local field line displacement and is energy independent. The energy-dependent parts of (44) and (45) may be negligible in comparison with the compressional contributions (2) and (4), respectively. Note that (2) is of the order of $\mu\omega b_{||}$, while (44) is of the order of $\mu E_\phi/L_\perp$ is the scale on which the ambient magnetic field varies in the meridian ($L_\perp \sim R_E L/3$ for a dipole field). Equation (40) allows one to relate $b_{||}$ to E_ϕ in terms of l_n, the scale of variation of the wave field in the meridian plane on an order of magnitude basis as

$$|\omega b_{||}| \sim |E_\phi/l_n| \tag{46a}$$

Thus the inequality

$$l_n < L_\perp \tag{46b}$$

provides a guide (which, however, is neither strictly sufficient or necessary) for the neglect of terms proportional to $\dot{W}_E$, i.e., it implies

$$\dot{W}_E < \dot{W} \tag{47}$$

We shall assume this inequality in the remainder of this paper, and therefore we omit contributions proportional to $\dot{W}_E$, calculating the change of energy from $\dot{W}$ of (2). The inequality (47) also allows us to simplify the calculation of radial velocity. This can be seen from (4) and (2), which yield

$$|\dot{L}| = \left|\frac{\mu m b_{||}}{qB_e L R_E^2}\right| = \left|\frac{m\dot{W}}{q\omega B_e L R_E^2}\right|$$

It follows that the magnitude of $\dot{L}$ exceeds that of the second term of (45) by a factor $|\dot{W}/\dot{W}_E|$. When (47) holds, the radial velocity $\dot{L} + \dot{L}_E$ may be approximated using

$$\dot{L}_E \simeq \frac{d}{dt}(\boldsymbol{\xi} \cdot \nabla L) \tag{48}$$

Neglect of (44) and use of (48) in place of (45) implies that direct compressional effects and possibly field line displacement dominate the wave. In the other extreme limit, with $\dot{W}_E \gg \dot{W}$, E_ϕ effects are completely dominant. Then the treatment of paper 1 (for transverse waves) is appropriate, as the negligible terms in $b_{||}$ are the only ones specific to a compressional signal.

7. SUMMARY OF THEORETICAL PREDICTIONS

In the preceding sections we have reviewed the major effects that a compressional ULF magnetic signal could produce in a particle flux. We have assumed that the particles are sufficiently energetic that the particle bounce frequency exceeds or is of the order of the wave frequency, which allowed us to

TABLE 1. Response of Particle Flux to Compressional Waves, With $\omega_b \gg m\bar{\omega}_d$, ω Unless Otherwise Noted

	$\omega \sim \omega_b$	$\omega > m\omega^*$, $m\bar{\omega}_d$	$\omega \sim m\omega^*$	$\omega \sim m\bar{\omega}_d$	$m\bar{\omega}_d > \omega$, ω^*	$\omega_b \sim m\bar{\omega}_d$
Symmetric	B, $M^{a,b}$	B, M^b	M	R, B^c	M	M^a
Antisymmetric	R	M	M	M^a	M	R

[a] Resonance inoperative.
[b] Mirror effect dominant if $b_{\|0} \ll b_{\|}$, otherwise betatron.
[c] If distribution is adiabatic ($\omega_d = \omega^*$), resonant terms cancel. Response is then B or M; see preceding footnote.

ignore gyration effects considered in paper 1. The explicit results of sections 2–5 ignore other electric field effects, including those associated with $E \times B$ motion of a particle gradient normal to B in the meridian. Writing l_f for the distribution gradient scale in L shell and using (43) for order of magnitude estimates of how $b_{\|}$ and ξ scale (see also (46b)), one concludes that if $l_f < l_n$, the convective term will dominate and the expressions we have given in sections 2 to 5 would require modification.

Conditions under which it is inappropriate to neglect the $E \times B$ motion of the particle gradient can be obtained by comparing expressions such as (15)–(17), (22), (32), and (36) with $\delta f \simeq -\xi \cdot \nabla f$, the change in f related to $\dot{L}_E$ of (48).

As a summary of the results when convection by the wave electric field is unimportant, we have drawn up Table 1. Three types of behavior are important. We have classified these as B (perpendicular or betatron heating), M (mirror effect, quasi-static response), and R (resonant response). Most commonly near geostationary orbit, the particle distributions fall off monotonically with perpendicular energy. Then category B flux oscillations will be in phase with $b_{\|}$. At fixed energy, the distribution often decreases monotonically with pitch angle away from 90°. For such distributions, category M flux oscillations will be in antiphase with $b_{\|}$. The resonant response, R, is complicated. First, note that as the first footnote of the table indicates, the important resonances are a function of wave symmetry about the equator. When resonance effects are important, there will be some phase difference other than 0° or 180° between $b_{\|}$ and the flux oscillations. The phase difference is a function of the range of energy to which the detector responds relative to the energy at which strict resonance occurs (see paper 1 for details).

8. ON SELF-CONSISTENCY AND RESONANT RESPONSE

Before discussing observations, one question concerning self-consistency should be addressed. We have been treating field and particle distributions as if they were unconnected. In a full description of wave phenomena that is not possible. In particular, there is a strong interaction between waves and resonant particles which can be viewed as causing diffusion in phase space, during which energy is exchanged between waves and particles [*Southwood*, 1980]. If the source of wave energy is the resonant particles themselves, then in equilibrium the particle energy lost in resonant diffusion balances the wave energy lost by, say, radiation or some other damping process. A consequence of this notion is that where there are few wave-damping mechanisms, the net resonant diffusion associated with an instability that has equilibrated will be slight, as little energy is required to maintain the waves [*Southwood*, 1983]. The diffusion coefficient is proportional to the wave power and will not go to zero with equilibration. Rather, the distri-

bution gradient along the phase space diffusion path will tend to zero. One may confirm (see, e.g., *Southwood* [1980]) that the relevant gradient is the combination of spatial (through ω^*) and energy gradients multiplying the resonant term in, say, (25) or (39). In such circumstances, the characteristic in-quadrature resonant response will be small.

9. OBSERVATIONS

In this section we examine some well-documented examples of particle responses to compressional waves to illustrate applications of ideas developed in preceding sections. An early attempt to model particle flux responses to field compressions was made by *Lin et al.* [1976]. They modeled flux oscillations in electrons with greater than 50-keV energy recorded on the geosynchronous ATS 1 spacecraft. They used the locally observed magnetic signal and assumed that the amplitude did not vary over the particle bounce orbit. Such a disturbance falls into our symmetric category. Evidently, in the absence of any assumption with respect to spatial variation, condition (A8) is satisfied, and we would predict flux and field strength oscillations in phase just as Lin et al. do. As *Lin et al.* [1976] report that there is a class of events for which their simple model works, we conclude that instances of betatron heating dominating particle response to compressional modes are common.

Instances of the mirror effect response are also commonly reported, as for example in the recent important work of *Kremser et al.* [1981]. *Kremser et al.* [1981] also use data from geosynchronous orbit, in their case from the GEOS 2 spacecraft. Not only do they find ion and electron flux oscillations (at energies of ~20 keV) in association with compressional magnetic signals, but they also show that the relative phase between the particle flux oscillation and the magnetic signal depends on the particle pitch angle distribution. For pitch angle distributions peaked at right angles to B, flux and field were found to oscillate in antiphase. However, in some cases, the electron distributions peaked at small pitch angle, and then the phase relation seen between the electron flux and field oscillations was reversed.

Similar signals to those reported by *Kremser et al.* [1981] were also reported by *Brown et al.* [1968] and *Sonnerup et al.* [1969]. In these papers, energetic proton flux oscillations were observed in antiphase with the magnetic oscillations. Further studies by *Lanzerotti et al.* [1969] showed that in-phase energetic electron oscillations were present and indeed showed that the mirror effect explained what was seen.

The correlation between the relative phase of the particle and field oscillations and the sense of pitch angle anisotropy evident in the Kremser et al. results strongly suggests that the mirror effect dominates the wave response of both energetic electrons and ions in the events reported. That modulations
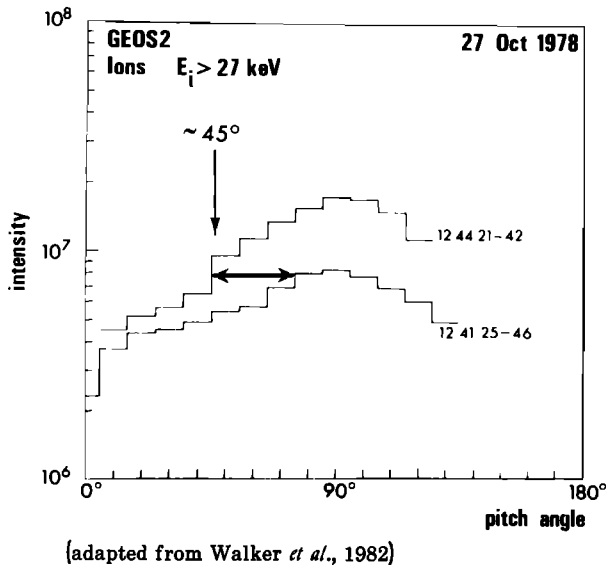
(adapted from Walker et al., 1982)

Fig. 2. Pitch angle distribution of ions >27 keV at field strength maximum (lower curve) and at a field strength minimum (upper curve) during the October 27, 1978, compressional wave event [Walker et al., 1982]. The 90° flux at field maximum is comparable with the 45° flux when the field is minimum.

are largest in the 90° channel is also consistent with the mirror effect.

Walker et al. [1982] study one of the *Kremser et al.* [1981] events in great detail. In Figure 2 we reproduce a plot given by them of the ion pitch angle distribution above 27-keV energy. The two curves shown are taken at the oscillation maximum and minimum. We have modified the original diagram by inserting a double arrow, which serves to indicate where the upper plot passes the maximum value attained by the lower. If the mirror effect is completely dominant, particle energy changes are insignificant, and it is possible simply to compute the particle pitch angle change between field maximum and minimum with the familiar formula used in a steady magnetic field, namely,

$$\sin^2 \alpha_{\min} = \frac{B_{\min}}{B_{\max}} \sin^2 \alpha_{\max} \qquad (49)$$

Subscripts have been introduced to denote values at maximum and minimum field. Taken with the statement, $f = \text{const}$, one has an extension of the linear treatment we have limited ourselves to when considering multiple effects. In the instance illustrated, $B_{\min} = 57$ nT and $B_{\max} = 103$ nT. The predicted pitch angle of a particle with 90° pitch angle when $B = B_{\max}$ is $\sim 48°$ when $B = B_{\min}$, giving good agreement with the point where the fluxes match. The full distribution at field maximum can be satisfactorily obtained from the 0°–48° measurements at field minimum, and the result is indeed consistent with expectations for a dominant mirror effect. It should be noted that this conclusion is independent of the details of wave structure or the generation mechanism (e.g., drift mirror instability, resonant particle-driven instability, etc.).

The data shown in Figure 2 are derived from integral measurements above 27 keV. Further data from *Walker et al.* [1982] are reproduced in adapted form in Figure 3. Shown are magnetic field oscillations (in the *V*, *D*, *H* coordinate system commonly used at synchronous orbit [*Kremser et al.*, 1981]), as well as flux oscillations at $\sim 90°$ pitch angle in three energy

channels and similar measurements at small pitch angle from one channel. The small amplitude of the signal in 28- to 36-keV particles with pitch angles of 28°–35° appears also consistent with the mirror effect if the pitch angle distribution for the lowest energy channel dominates the integral intensity plotted in Figure 2. From (48) it follows that near 30° the particle pitch angle varies by 10° between wave minimum and maximum. As Figure 2 shows a rather weak variation of intensity versus pitch angle near 30°, wave modulation would be difficult to detect.

For the two lower energy channels shown in Figure 3, flux oscillations are in antiphase with $b_{\parallel}$, as one expects if the background pitch angle distribution peaks at 90°. We have earlier noted that in-phase oscillations will occur if the pitch angle distribution increases away from 90°. In the most energetic channel plotted in Figure 3, the 75- to 98-keV channel, an antiphase flux oscillation is seen in the latter half of the data (1230–1300 UT), but the signature is more complex between 1200 and 1230 UT, where arguably the flux is oscillating at closer to twice the frequency of the field oscillation. The phase relation between the flux and field signal is fairly well fixed: the flux has minima when the field is both maximum and minimum.

The mirror effect can also be invoked to explain the rather complicated field and particle flux coupling evident in the 75- to 98-keV channel. As indicated in the calculation presented above, large changes in pitch angle are produced between field maxima and minima in a signal as large as that being considered. Should the pitch angle distribution vary other than monotonically over the range through which the wave induces pitch angle changes, the flux oscillation will reflect the variation. Let us say that the particles with 90° pitch angle when the field is maximum have pitch angle α_M when the field is minimum. Now consider a background pitch angle distribution with a maximum at a pitch angle between 90° and α_M, as illustrated in Figure 4a. When the field is maximum and minimum, the detector will detect a flux proportional to the distribution at α_M and 90°, respectively. At other times, it will detect the flux corresponding to the distribution at intermediate pitch angles. In the original distribution the flux increases as one moves to lower pitch angle from 90° and to higher pitch angle from α_M, so local minima in flux will occur when the field is at both a maximum and a minimum. A signal such as we show in Figure 4b results.

It is clear from the above that the mirror effect can explain all the oscillations shown in Figure 3 if the background pitch angle distribution in the most energetic channel is as illustrated in Figure 4a, i.e., it peaks off the plane perpendicular to **B**. We do not have sufficient pitch angle information to test this hypothesis; thus it remains a prediction. Distributions of the form predicted are reported at synchronous orbit in the appropriate energy range. For example, *Kaye et al.* [1978] show cases where nonmonotonic distributions appear only in one channel and are also present only intermittently. We would require that the nonmonotonicity had disappeared at ~ 1230 UT, where the high-frequency modulation disappears.

The interpretation of the wave event of October 27, 1978, in terms of the mirror effect clearly has many strengths. The circumstances under which the mirror effect is dominant depend on the symmetry of the wave. As Table 1 shows, there are three circumstances under which one expects the mirror effect to be dominant in a symmetric signal: (1) when $m\tilde{\omega}_d \gg \omega$, (2) when $\omega \sim m\omega^*$, and (3) when $\omega \gg m\tilde{\omega}_d$, $m\omega^*$ if $b_{\parallel 0} \ll b_{\parallel}$. The latter case can be rapidly ruled out. GEOS 2 is close to
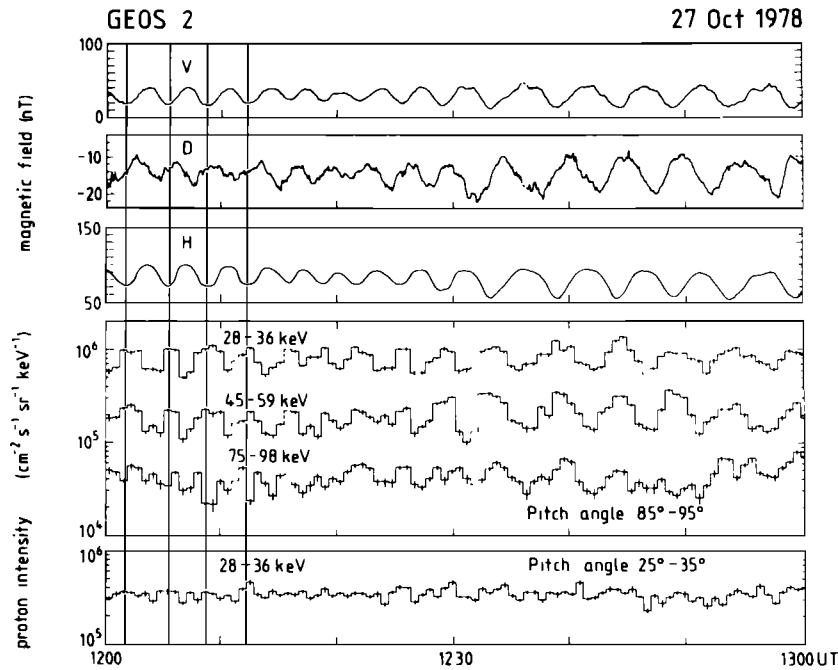
(adapted from Walker *et al.*, 1982)

Fig. 3. Three components, V, D, H, of magnetic field oscillations at GEOS 2, flux oscillations at $\sim 90°$ pitch angle in three channels, and one example of the signal in a small (25°–35°) pitch angle detector from GEOS 2 1200–1300 UT on October 27, 1978 (adapted from *Walker et al.* [1982]). (Note the scale differs for the D component.)

the equator, and we are examining particles mirroring locally which have bounce amplitudes extending only $\sim 4°$ off the equator. It would be unreasonable to argue that the bounce average of $b_\parallel$ should be radically different from the local value.

There is a strong argument against $\omega \sim m\omega^*$ being the pertinent limit. Even if the local plasma distribution had ω^* independent of ion energy, condition 2 could not simultaneously hold for the energetic electron distribution. As defined in (7),

Fig. 4. (*a*) Example of a pitch angle distribution peaking off 90°; α_M is the minimum pitch angle attained by a particle which has 90° pitch angle when the field strength is maximum during an oscillation. (*b*) Field oscillations and the flux oscillations produced if the mirror effect is dominant, and the undisturbed distribution resembles that shown in Figure 4*a*.

the sign of ω^* is charge dependent. A characteristic of the *Kremser et al.* [1981] events is that the energetic electron response is also dominated by the mirror effect.

Limit 1, $m\bar{\omega}_d \gg \omega$, also raises problems, for *Walker et al.*'s [1982] ionospheric measurements allow estimation of the signal perpendicular wavelength and thus of ω/m. In fact, *Walker et al.* [1982] and *Allan et al.* [1982] point out that at geostationary orbit, $\bar{\omega}_d$ for a particle with an energy of about 40 keV in a dipole field satisfies $\bar{\omega}_d = \omega/m$ with the value of ω/m that they deduce. From this one would conclude that ~ 40-keV ions are resonant and they would not satisfy condition 1. Rather than the mirror effect, one might expect a quadrature resonant signature in the lower energy channels. The absence of such a signature may be attributable to the saturation of the driving instability mechanism as discussed in section 8 above. Alternatively, the low-energy ions may not be resonant because the dipole approximation may be inappropriate; the field is strongly distorted at the time of the event, with magnitude depressed by more than 25% from its dipole value. In such circumstances, it seems reasonable that the field gradient at synchronous orbit may be substantially increased over its dipole value. Were it doubled, the resonance would be removed from the range of Kremser et al.'s detectors (energy > 22 keV for ions, 27 keV for electrons), and condition 1 could apply within the measured range for both species.

If, on the other hand, the signal is not symmetric but rather antisymmetric, then the dominance of the mirror effect can easily be explained. As Table 1 shows, the mirror effect is expected in antisymmetric waves unless resonance effects are important.

Let us now examine the symmetry of the wave in the light of all the information that has been provided for this event. In addition to *Kremser et al.* [1981] and *Walker et al.* [1982], three other papers have been published [*Allan et al.*, 1982,
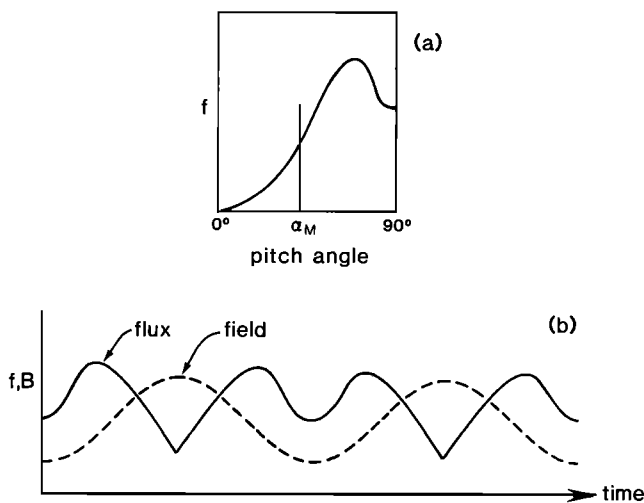
1983; *Walker et al.*, 1983]. In the latter paper, the year of the event is erroneously given as 1979. *Walker et al.* [1982] showed simultaneous measurements of the ionospheric electric field signal during the disturbance, thus demonstrating that the wave is present all along the field. A standing structure seems reasonable. They concluded that the signal is symmetric, basing the argument on the fact that the compressional magnetic field component $b_{||}$ exceeds B_n, the meridional field perturbation perpendicular to **B**, with $b_n/b_{||} \sim 0.3$. A symmetric signal would have a node in b_n at the equator and an antinode in $b_{||}$. The reverse applies to an antisymmetric signal. GEOS 2 is very close to the equator ($\sim 4°$ southern latitude). It seems unreasonable to claim $b_{||}$ could have a node nearby. The $b_n/b_{||}$ ratio observed strongly suggests that the signal is symmetric.

A completely different conclusion regarding wave symmetry was drawn in a subsequent paper by *Walker et al.* [1983]. Their modified conclusion is based on evidence obtained from measurements of the drift velocity of 1.2-keV electrons from the GEOS 2 electron gun experiment. Oscillations of the V component of the drift velocity (u_v) are identified and are found to lag $b_{||}$ and b_v by 90°. *Walker et al.* [1983] argue that the observed phase relation is inconsistent with expectations for a symmetric standing wave observed below the magnetic equator. They propose that b_n is associated with a transverse antisymmetric structure, while $b_\phi(D)$ and $b_{||}$ are associated with a symmetric structure, which couples with the transverse signal. It is intuitively hard to see how such a coupling could be achieved. The result thus remains somewhat puzzling.

Symmetry is also discussed in the paper by *Allan et al.* [1983], who compare the amplitudes of the magnetic signal seen on the ground and the transverse signal seen on GEOS 2. They conclude that the amplitude distribution differs strongly from that calculated for a standing toroidal transverse mode [*Allan and Knox*, 1979] but recognize that the compressional features observed are not dealt with by that theory.

On balance, despite the uncertainties in the interpretation of the full data set, we regard the measured magnetic field amplitudes as very persuasive and therefore favor the interpretation based on symmetric structure in $b_{||}$, with a departure from dipolar field to allow $m\bar{\omega}_d \gg \omega$. As we next show, there are other types of signal recorded at synchronous orbit where the field evidence points to the compression being antisymmetric.

Our final example of compressional wave flux oscillations also comes from data recorded at synchronous orbit. In Figure 5, we show data from the ATS 6 spacecraft from a 1-hour interval on June 29, 1974. The magnetometer data are from the University of California, Los Angeles, instrument on the spacecraft. The particle count rates (courtesy of T. A. Fritz) are from the C telescope of the Low-Energy Proton Experiment, which was viewing at an angle of 103°–110° with respect to **B** during the hour. The amplitude of the oscillations (~ 120-s period) peaks in the 100- to 151-keV channel, both as plotted or in terms of fractional change in the count rate for each channel. Similar oscillations were present in the count rates of telescopes oriented at $\sim 60°$ and $\sim 30°$ to **B**. The period (~ 120 s) is considerably shorter than that in the GEOS 2 event discussed above.

The event is typical of a class of events identified by *Higbie and McPherron* [1982]. An important feature of these signals is that they appear to occur near the second harmonic of azimuthally polarized standing Alfvén wave signals. This property is illustrated in Figure 6, which displays the dynamic spectra of the three magnetic field components V, D, H for a
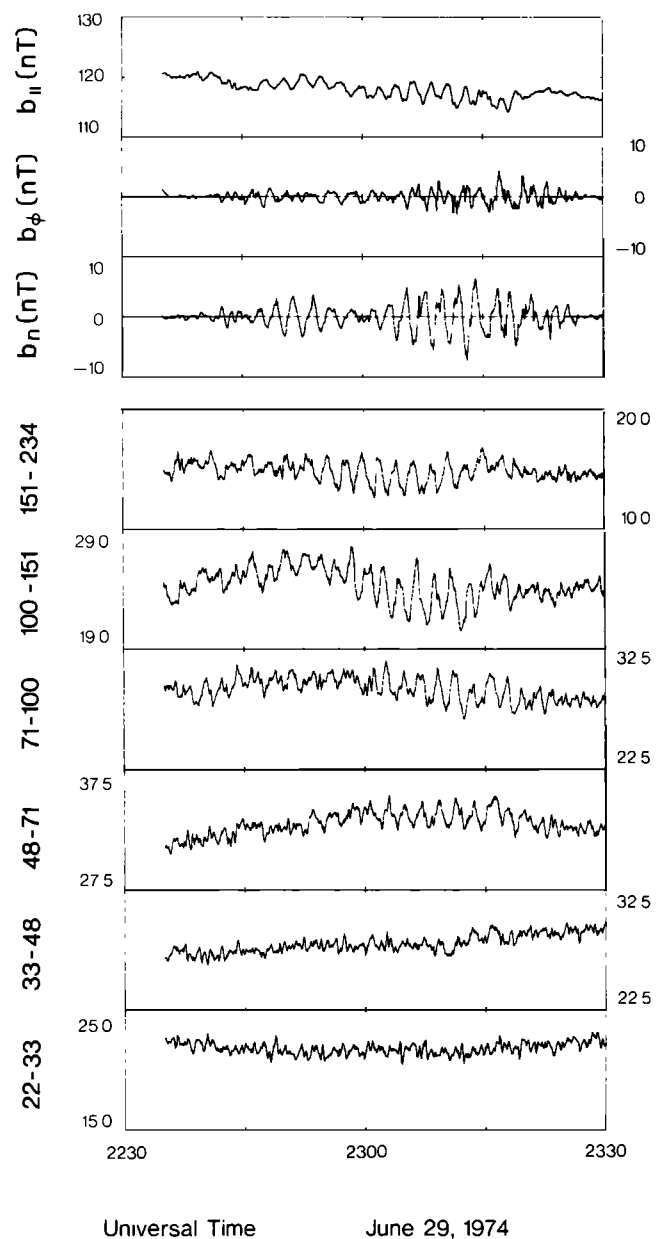
Universal Time   June 29, 1974

Fig. 5. Magnetometer data from the UCLA instrument on ATS 6 and particle data (courtesy of T. A. Fritz) from the C telescope of the Low-Energy Proton Experiment on the same spacecraft. The field data have been rotated into a coordinate system aligned with ambient field. The R axis points away from earth perpendicular to **B**, and ϕ completes the set. The energy channel is labeled on the left-hand side of each panel of particle data. Count rate is plotted. (Data provided by P. Higbie.)

24-hour period from 0600 UT on June 29, 1974. The corresponding local time range starts at 0000. The spectra (kindly provided by K. Takahashi) follow the format pioneered by *Takahashi and McPherron* [1982]. Although clearer examples are given in their paper, several of the features of synchronous orbit ULF wave behavior pointed out by *Takahashi and McPherron* [1982] are present in Figure 6. For most of the dayside hours (~ 1200–2400 UT), dominant activity is in the D component (central panel). (The high power at very low frequencies should be ignored.) A band with slowly decreasing frequency is very evident between 1200 and 2000 UT. This band is identifiable as the third-harmonic signal. Signals at second and fourth harmonics are just perceptible. The com-
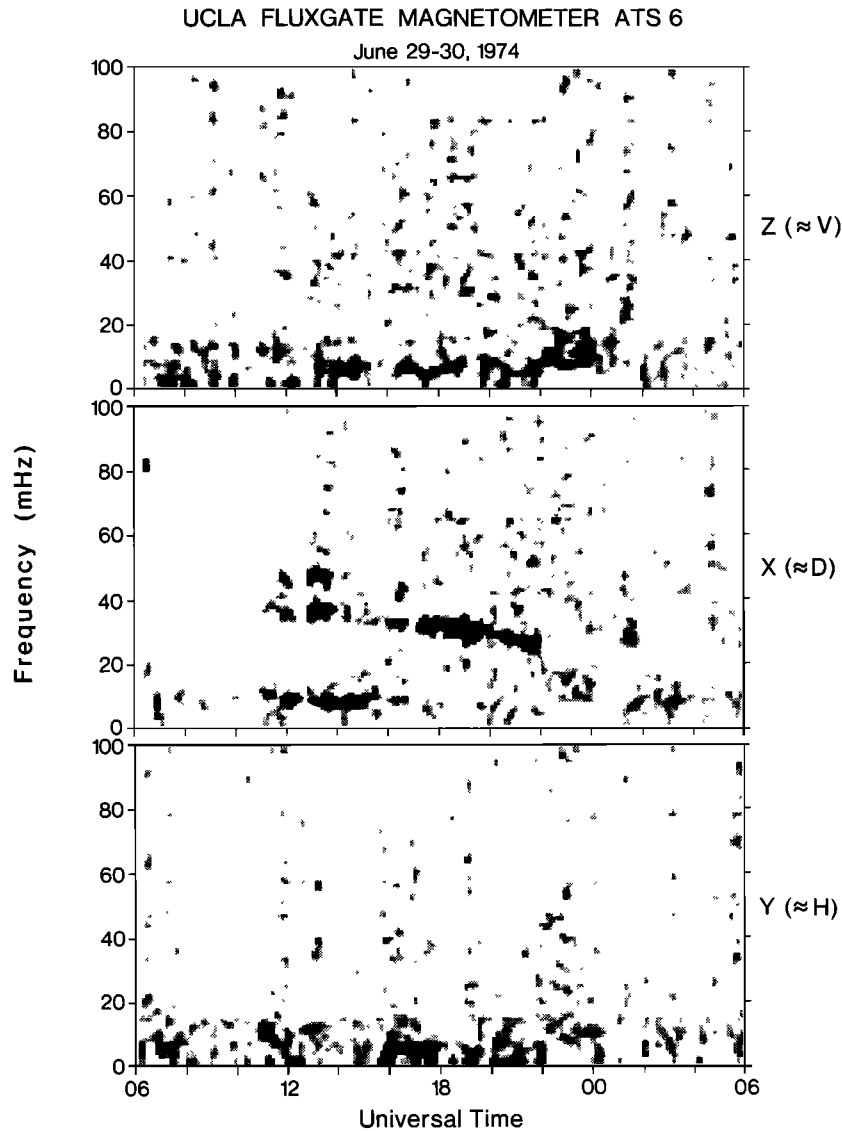
UCLA FLUXGATE MAGNETOMETER ATS 6
June 29-30, 1974

Fig. 6. Dynamic spectra of V, D, H magnetic components from ATS 6 for the 24-hour period commencing at 0600 UT on June 29, 1974 (provided by *Takahashi and McPherron* [1982]).

pressional event is seen between 2000 and 2200 UT and shows up in all three panels at a frequency below the temporarily suppressed third-harmonic signal. The compressional signal is in the frequency band identified as the second harmonic of the earlier azimuthal oscillations. The occurrence of signals near the second harmonic in the late afternoon is a characteristic of the events identified by *Higbie and McPherron* [1982]. Several papers have suggested that compressional signals in an inhomogeneous medium may be controlled by the natural standing wave frequencies of Alfvén waves [*Southwood*, 1976, 1977; *Lin and Parks*, 1978; *Walker et al.*, 1982; *Southwood and Kivelson*, 1984]. Any compressional component associated with second-harmonic Alfvén wave structure would be expected to be antisymmetric about the equator.

The ATS 6 spacecraft is at 10° latitude and thus is farther from the equator than GEOS. However, we expect that the relative size of the amplitudes b_n and $b_{||}$ at the spacecraft should still reflect whether they have nodal or antinodal behavior at the equator. In this case, $|b_n/b_{||}|$ is of order 3; thus it seems likely that $b_{||}$ has a node, and the wave is anti-

symmetric. The oscillations shown in Figure 6 differ significantly from the *Walker et al.* [1982] event discussed above. The oscillations are barely detectable in the low energy channels illustrated, and they peak in the second highest energy channel (100–150 keV) shown. Although there can be no doubt particles are responding to the field oscillations, the phase relationship between flux and field oscillations is a function of energy.

Figure 7 further illustrates the field-flux phase relation. It is easiest to define the relative phase between the transverse, b_n, component and the count rate at each energy, but note that b_n is in strict antiphase with $b_{||}$ (see Figure 5). In Figure 7, we show a plot (kindly provided by P. Higbie) of the relative phase as a function of energy for the C telescope (used in Figure 5) and also for the A and B telescopes. The latter telescopes provide data for smaller pitch angles. Figure 7 shows that there is a systematic shift of phase through the energies where the oscillation amplitude is greatest. For the particles entering the C telescope, the phase relations relative to b_n shift from in phase to approximately in antiphase across
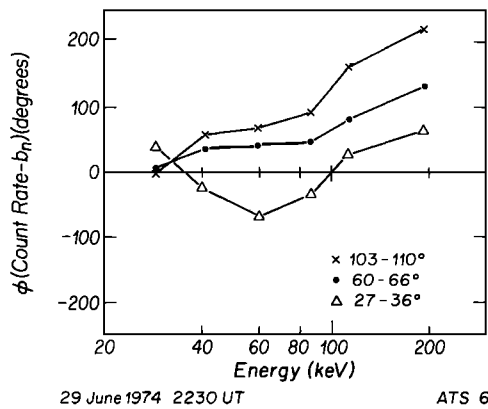
Fig. 7. Phase difference between count rate and the meridional field component, b_n, versus energy channel for the three low-energy proton telescopes on ATS 6 for the June 29, 1974, event. The pitch angle coverage of each telescope is indicated in the lower right-hand corner.

the range of energies measured. Such a shift is expected (e.g., (29) or (31)) across a resonant energy. Near 100 keV it seems the response is in quadrature, so according to our earlier work this channel contains particles resonating with the wave. With the likely antisymmetric nature of the signal in mind, it is natural to consider the resonance given by $\omega - m\tilde{\omega}_d = \pm\omega_b$. Particles with energy 100 keV satisfy the high-energy resonance (using a dipole field model), $m\omega_d \sim \omega_b$, provided $m \sim 140$. It is interesting to note that if this is so, lower-energy particles with $\omega \sim \omega_b$ would also be in resonance, the resonant energy being of the order of 3–5 keV. The University of California, San Diego (UCSD), Auroral Particle Experiment on ATS 6 measures in this range [*Mauk and McIlwain*, 1975]. Sadly, the measurements at any particular energy on this experiment are repeated only every 24 s; thus it is very hard to detect a clear signature of a 100-s wave. Further study is planned using the UCSD data, but suffice it for now to note that there is evidence of modulation in the keV energy range. Furthermore, the background distribution near those energies shows evidence of nonmonotonic variation with energy ($\partial f/\partial W > 0$). *Southwood* [1980] points out that such a distribution can be a source of wave energy.

A feature of the data in Figure 7 that we have yet to touch on is the clear phase difference among count rates in the three telescopes. The telescopes look in three different directions. In particular, with respect to the meridian plane, the C telescope looks to the west, A is in the meridian, and B looks to the east. If the wave phase varies significantly over the Larmor orbit, the phase difference between detectors can be explained, as *Su et al.* [1977] point out, by recognizing that detectors sample particles whose gyrocenters are displaced to the east or west of the spacecraft. The effect is discussed in detail in paper 3. Now, the value of m deduced above ($m \sim 140$) implies an east-west wavelength of ~ 1900 km. The Larmor radius of 100-keV particles is of the order of 500 km at synchronous orbit. It thus seems entirely reasonable that the phase difference be attributable to the finite Larmor radius effect.

In conclusion, we feel that in the June 29, 1974, event, we have a wave which is antisymmetric with respect to the equator. The particle response is symptomatic of bounce resonance effects being dominant with resonant particles with ~ 100 keV being in the high-energy resonance $m\tilde{\omega}_d \sim \omega_b$ and particles with energy near 1 keV being in low-energy resonance. The

wavelength is of the order of 1900 km at the equator, and thus finite Larmor radius effects as discussed in paper 3 are also evident.

It may well be that the June 29, 1974, event, and no doubt other *Higbie and McPherron* [1982] events, is generated by resonantly driven instability (*Southwood* [1980]; cf. also *Hughes et al.* [1978, 1979]). The reason that the resonant signature is not suppressed (as we suggested it could be in section 6 of this paper) may be the existence of two sets of resonant particles. Energy may be fed between the two sets of ions in resonance. There will also be a low-energy set of resonant electrons for which $\omega \sim \omega_b$, which will absorb energy from the wave. Note, in contrast, that in a symmetric signal in which drift resonance is dominant, there is only one set of resonant particles, those whose drift matches the perpendicular angular phase velocity.

10. DISCUSSION

We have outlined systematically the effects a low-frequency ($\omega < \omega_b$) compressional signal can produce in energetic particle flux. In a series of different limits, several forms of characteristic behavior recurred, corresponding to the dominance of either betatron, mirror, resonant, or convective effects. The first three are the most important, and instances of all three were described in the observations in section 7.

The conclusions we drew from the events we studied in detail for this paper were contingent on the assumed symmetry of the signal about the equator. In our reexamination of the GEOS 2 event analyzed by *Walker et al.* [1982], we concluded that the signal was likely to be symmetric. As we also concluded that the mirror effect was dominant, strong constraints were placed on how the particles were interacting with the wave. Testing for the mirror effect is straightforward, for not only does it not change the particle energy, but it also depends only on the local field strength and not on wave properties far from the spacecraft. Given pitch angle distribution information for each separate energy channel, a more stringent test can be done which would be worthwhile.

Establishing experimentally that there are classes of compressional waves for which both electron and ion responses are dominated by the mirror effect, as seems to occur in the *Kremser et al.* [1981] events, is significant for any theoretical description of the excitation mechanism. Evidence of this sort can be used as a constraint on self-consistent treatment of fields and particles. Clearly, with very wide energy and pitch angle coverage, particle flux behavior can be used as a very full diagnostic of signal structure. One could envisage such data being used as starting points for theory; unfortunately, spacecraft measurements often fail to give sufficiently complete coverage of both energy and pitch angle. Furthermore, as in the case of the ATS 6 data sets to which we referred above, the time resolution of measurements is inadequate. It is particularly frustrating in the ATS 6 instance, for we feel that we have clearly identified bounce resonance behavior in the energetic particle data set. Ingenious methods of analyzing the UCSD ATS 6 particle data have been used in the past by *Hughes et al.* [1979], and we plan further investigations. Other well-documented examples of ULF waves would be valuable for further tests of wave theory.

APPENDIX: THE MIRROR EFFECT AND THE BETATRON EFFECT

As a particle moves through a compressional wave conserving its first adiabatic invariant, μ, its energy, W, changes ac-

cording to the requirement that

$$\dot{W} = \mu \frac{\partial b_\parallel}{\partial t} \qquad (A1)$$

while its perpendicular energy, $W_\perp$, changes according to the requirement that $\mu = \text{const} = W_\perp/B_T$ where B_T is the total (unperturbed + perturbed) field strength. In a linear approximation,

$$\dot{W}_\perp = \mu \frac{dB}{dt} + \mu \frac{db_\parallel}{dt} \qquad (A2)$$

If the particle's total velocity is v, then

$$\frac{d}{dt} = \frac{\partial}{\partial t} + \mathbf{v} \cdot \nabla$$

and (2) may be rewritten

$$\dot{W}_\perp = \mu \mathbf{v} \cdot \nabla B + \frac{\partial b_\parallel}{\partial t} + \mu \mathbf{v} \cdot \nabla b_\parallel \qquad (A3)$$

The first term on the right-hand side of (A3) is independent of the disturbance signal and represents the fact that in steady state as a particle moves along the background field, B, energy is transferred between perpendicular and parallel motion by the magnetic field inhomogeneity. One deduces from (A1) and (A3) that the parallel energy varies as

$$\dot{W}_\parallel = -\mu \mathbf{v} \cdot \nabla B - \mu \mathbf{v} \cdot \nabla b_\parallel \qquad (A4)$$

Equations (A3) and (A4) show that in a low-frequency signal (1) one must allow for changes in both parallel and perpendicular energy, (2) energy is continually transferred between perpendicular and parallel motion as the particle moves through the background field, and (3) in the absence of electric field effects, it is actually time variation at a fixed position (see (A1)) that produces any net change in total energy. A corollary of 3 is that if a particle moves through the compressional signal so fast that the variations it sees satisfy

$$\frac{d}{dt} \simeq \mathbf{v} \cdot \nabla \gg \frac{\partial}{\partial t} \qquad (A5)$$

no net change in energy occurs, although energy is shifted between perpendicular and parallel components just as it is in motion through the background steady field. If (A5) applies, and in a time t the particle moves along the background field B from a point where $|\mathbf{B}| = B_1$, $b_\parallel = b_{\parallel 1}$ to where $|\mathbf{B}| = B_2$, $b_\parallel = b_{\parallel 2}$, respectively, then $W_\perp$ and $W_\parallel$ change by amounts $\delta W_\perp$, $\delta W_\parallel$, respectively, where

$$\delta W_\perp = \mu(B_2 - B_1) + \mu(b_{\parallel 2} - b_{\parallel 1}) \qquad (A6a)$$

$$\delta W_\parallel = -\mu(B_2 - B_1) - \mu(b_{\parallel 2} - b_{\parallel 1}) \qquad (A6b)$$

Now, as particles move, they remain on the same contour of the phase space distribution function, f (Liouville's theorem). Hence in the above instance, if $\delta W_\perp$ and $\delta W_\parallel$ are small, the distribution function at a given energy differs between the two points in phase space by an amount

$$f_2 - f_1 = \mu(B_2 - B_1)\left(\frac{\partial f}{\partial W_\parallel} - \frac{\partial f}{\partial W_\perp}\right)$$

$$+ \mu(b_{\parallel 2} - b_{\parallel 1})\left(\frac{\partial f}{\partial W_\parallel} - \frac{\partial f}{\partial W_\perp}\right) \qquad (A7)$$

The first term in (A7) is present even in the absence of a

disturbance; the second term arises from the compressional signal. Note in particular that in the quasi-static limit represented by condition (A5), the distribution function is different at two points where $B_1 = B_2$, but $b_{\parallel 1} \neq b_{\parallel 2}$. Equally well if one considers what happens at two different times between which $b_\parallel$ changes, the distribution is changed. In general, at any particular point in space, even in the absence of changes in particle energy, there will be a portion of the distribution function that varies proportionally to the local value of $b_\parallel$ unless the original distribution is isotropically distributed in pitch angle, i.e., unless

$$\frac{\partial f}{\partial W_\parallel} = \frac{\partial f}{\partial W_\perp}$$

Condition (A5) represents an extreme; the opposite extreme is when time variation dominates the changes in $b_\parallel$ seen by the particle

$$\frac{\partial}{\partial t} \gg \mathbf{v} \cdot \nabla \qquad (A8)$$

When condition (A8) holds, the energy changes, and, moreover, the energy change is entirely in the perpendicular component, for

$$\dot{W} = \mu \frac{\partial b_\parallel}{\partial t} \simeq \mu \frac{db_\parallel}{dt} = \frac{dW_\perp}{dt} \qquad (A9)$$

The energy rises and falls in phase with $b_\parallel$. As the spatial derivatives are unimportant (condition (A8)), inhomogeneity is not effective in transferring perpendicular to parallel energy. The local change in distribution in this case is evidently

$$\delta f = -\mu b_\parallel \frac{\partial f}{\partial W_\perp} \qquad (A10)$$

For any condition between (A5) and (A8), W and both $W_\parallel$ and $W_\perp$ vary in response to a compressional signal. However, when considering the response of the distribution function to a wave disturbance with arbitrary $\mathbf{v} \cdot \nabla/\partial t$, it is advantageous to replace the parameters $W_\parallel$ and $W_\perp$ by coordinates that are constant during the undisturbed adiabatic motion. An obvious pair of coordinates to replace $W_\parallel$, $W_\perp$ are μ, W. Evidently

$$\delta W = \delta W_\perp + \delta W_\parallel$$

$$\left.\frac{\partial}{\partial W}\right|_\mu = \left.\frac{\partial}{\partial W_\parallel}\right|_{W_\perp} \qquad \left.\frac{\partial}{\partial \mu}\right|_W = B\left(\frac{\partial}{\partial W_\perp} - \frac{\partial}{\partial W_\parallel}\right) \qquad (A11)$$

If the distribution is uniform across the field, the linear change in a distribution function produced by a small change in field equal to $b_\parallel$ is given by

$$\delta f = -\delta W_\perp \left.\frac{\partial f}{\partial W_\perp}\right|_{W_\parallel} - \delta W_\parallel \left.\frac{\partial f}{\partial W_\parallel}\right|_{W_\perp}$$

$$= -\delta W_\perp \left(B^{-1} \left.\frac{\partial f}{\partial \mu}\right|_W + \left.\frac{\partial f}{\partial W}\right|_\mu\right) - \delta W_\parallel \left.\frac{\partial f}{\partial W}\right|_\mu$$

$$\delta f = -\frac{\mu b_\parallel}{B} \left.\frac{\partial f}{\partial \mu}\right|_W - \frac{\mu \delta B_T}{B} \left.\frac{\partial f}{\partial \mu}\right|_W - \delta W \left.\frac{\partial f}{\partial W}\right|_\mu \qquad (A12)$$

In (A12), δB_T corresponds to a change of field magnitude with spatial displacement. For observations at a fixed spatial location $\delta B_T = 0$, and at constant particle energy (as would occur if condition (A5) held),

$$\delta f = -\frac{\mu b_\parallel}{B} \left.\frac{\partial f}{\partial \mu}\right|_W \qquad (A13)$$

Note that this change does not arise from changes in μ as it might appear, but from the fact that velocity space coordinates now scale as a function of the total magnetic field. The change in distribution represents the effect of particles being excluded from regions of stronger magnetic field by the mirror effect as they move through a quasi-static compressional field perturbation. We shall label the response represented by (A13) the "mirror effect" and shall find that in several situations it is the dominant particle response.

When time variation dominates, as when (A8) is satisfied,

$$\delta W = \mu b_\parallel \qquad (A14)$$

and with $\delta B_T = 0$, (A12) becomes

$$\delta f = -\mu b_\parallel \left(\frac{1}{B} \frac{\partial f}{\partial \mu} + \frac{\partial f}{\partial W} \right) \qquad (A15)$$

Using (A11), one may show that indeed this corresponds to (A10), and it is this response that we describe as the "betatron effect."

REFERENCES

Allan, W., and F. B. Knox, The effect of finite ionospheric conductivities on axisymmetric toroidal Alfvén wave resonances, *Planet. Space Sci., 27*, 939, 1979.

Allan, W., E. M. Poulter, and E. Neilsen, Stare observations of a Pc 5 pulsation with large azimuthal wave number, *J. Geophys. Res., 87*, 6163, 1982.

Allan, W., E. M. Poulter, K.-H. Glassmeier, and E. Neilsen, Ground magnetometer detection of a large-*m* pulsation observed with the Stare radar, *J. Geophys. Res., 88*, 183, 1983.

Barfield, J. N., and R. L. McPherron, Storm time Pc 5 magnetic pulsations observed at synchronous orbit and their correlation with the partial ring current, *J. Geophys. Res., 83*, 739, 1978.

Brown, W. L., L. J. Cahill, L. R. Davis, C. E. McIlwain, and C. S. Roberts, Acceleration of trapped particles during a magnetic storm on April 18, 1965, *J. Geophys. Res., 73*, 153, 1968.

Dungey, J. W., Effects of electromagnetic perturbations on particles trapped in the radiation belts, *Space Sci. Rev., 4*, 199, 1965.

Hasegawa, A., *Plasma Instabilities and Nonlinear Effects*, Springer Verlag, New York, 1975.

Higbie, P. R., and R. L. McPherron, A class of radially polarized Pc 3–4 events (abstract), *Eos Trans. AGU, 63*, 415, 1982.

Hughes, W. J., D. J. Southwood, B. Mauk, R. L. McPherron, and J. N. Barfield, Alfvén waves generated by an inverted plasma energy distribution, *Nature, 275*, 43, 1978.

Hughes, W. J., R. L. McPherron, J. N. Barfield, and B. H. Mauk, A compressional Pc 4 pulsation observed by three satellites in geostationary orbit near local midnight, *Planet. Space Sci., 27*, 821, 1979.

Kaye, S. M., C. S. Lin, G. K. Parks, and J. R. Winckler, Adiabatic modulation of equatorial pitch angle anisotropy, *J. Geophys. Res., 83*, 2675, 1978.

Kivelson, M. G., and D. J. Southwood, Charged particle behavior in low-frequency geomagnetic pulsations, 3, Spin phase dependence, *J. Geophys. Res., 88*, 174, 1983.

Kremser, G., A. Korth, J. A. Fejer, B. Wilken, A. V. Gurevich, and E. Amata, Observations of quasi-periodic flux variations of energetic ions and electrons associated with Pc 5 geomagnetic pulsations, *J. Geophys. Res., 86*, 3345, 1981.

Lanzerotti, L. J., A. Hasegawa, and C. G. Maclennan, Drift mirror instability in the magnetosphere: Particle and field oscillations and electron heating, *J. Geophys. Res., 74*, 5565, 1969.

Lin, C. S., and G. K. Parks, The coupling of Alfvén and compressional waves, *J. Geophys. Res., 83*, 2628, 1978.

Lin, C. S., G. K. Parks, and J. R. Winckler, The 2- to 12-min quasi-periodic variation of 50- to 1000-keV trapped electron fluxes, *J. Geophys. Res., 81*, 4517, 1976.

Mauk, B. H., and C. E. McIlwain, UCSD auroral particles experiment, *IEEE Trans. Aerosp. Electron. Syst., 11*, 1125, 1975.

Northrop, T. G., *The Adiabatic Motion of Charged Particles*, p. 12, Wiley Interscience, New York, 1963.

Saunders, M. A., D. J. Southwood, E. Hones, Jr., and C. T. Russell, A hydromagnetic vortex seen by ISEE 1 and 2, *J. Atmos. Terr. Phys., 43*, 927, 1981.

Saunders, M. A., D. J. Southwood, T. A. Fritz, and E. W. Hones, Jr., Hydromagnetic vortices, 1, The December 11, 1977 event, *Planet. Space Sci., 31*, 1099, 1983a.

Saunders, M. A., D. J. Southwood, and E. W. Hones, Jr., Hydromagnetic vortices, 2, Further dawnside events, *Planet. Space Sci., 31*, 1117, 1983b.

Sonnerup, B. U. Ö., L. J. Cahill, Jr., and L. R. Davis, Resonant vibration of the magnetosphere observed from Explorer 26, *J. Geophys. Res., 74*, 2276, 1969.

Southwood, D. J., Behaviour of ULF waves and particles in the magnetosphere, *Planet. Space Sci., 21*, 53, 1973.

Southwood, D. J., A general approach to low-frequency instability in the ring current plasma, *J. Geophys. Res., 81*, 3340, 1976.

Southwood, D. J., Localised compressional hydromagnetic waves in the magnetospheric ring current, *Planet. Space Sci., 25*, 549, 1977.

Southwood, D. J., Low frequency pulsation generation by energetic particles, *J. Geomagn. Geoelectr., 32*, suppl. 2, 75–88, 1980.

Southwood, D. J., Wave generation in the terrestrial magnetosphere, *Space Sci. Rev., 35*, 259, 1983.

Southwood, D. J., and M. G. Kivelson, Charged particle behavior in low-frequency geomagnetic pulsations, 1, Transverse waves, *J. Geophys. Res., 86*, 5643, 1981.

Southwood, D. J., and M. G. Kivelson, Charged particle behavior in low-frequency geomagnetic pulsations, 2, Graphical approach, *J. Geophys. Res., 87*, 1707, 1982.

Southwood, D. J., and M. G. Kivelson, Relations between polarization and the structure of ULF waves in the magnetosphere, *J. Geophys. Res., 89*, 5523, 1984.

Southwood, D. J., J. W. Dungey, and R. J. Etherington, Bounce resonant interaction between pulsations and trapped particles, *Planet. Space Sci., 17*, 349, 1969.

Su, S.-Y., A. Konradi, and T. A. Fritz, On propagation direction of ring current proton ULF waves observed by ATS 6 at 6.6 R_E, *J. Geophys. Res., 82*, 1859, 1977.

Takahashi, K., and R. L. McPherron, Harmonic structure of Pc 3–4 pulsations, *J. Geophys. Res., 87*, 1504, 1982.

Walker, A. D. M., R. A. Greenwald, A. Korth, and G. Kremser, Stare and GEOS 2 observations of a storm time Pc 5 ULF pulsation, *J. Geophys. Res., 87*, 9135, 1982.

Walker, A. D. M., H. Junginger, and O. H. Bauer, GEOS 2 plasma drift velocity measurements associated with a storm time Pc 5 pulsation, *Geophys. Res. Lett., 10*, 757, 1983.

M. G. Kivelson and D. J. Southwood, Institute of Geophysics and Planetary Physics, University of California, Los Angeles, CA 90024.